

2013

Influence of annealing and thickness on the electrical properties of invar36 thin film for strain gauge applications

H. M Kalpana

Department of Instrumentation Technology, Siddaganga Institute of Technology, Tumkur 572103, Karnataka, India, kalpanaravi@yahoo.co.in

V. Siddeswara Prasad

Department of Instrumentation Technology, Siddaganga Institute of Technology, Tumkur 572103, Karnataka, India, kalpanaravi@yahoo.co.in

M. M Nayak

Centre for Nano Science and Engineering, Indian Institute of Science, Bangalore 560 012, India, kalpanaravi@yahoo.co.in

Follow this and additional works at: <https://digitalcommons.aaru.edu.fo/ijtfst>

Recommended Citation

M Kalpana, H.; Siddeswara Prasad, V.; and M Nayak, M. (2013) "Influence of annealing and thickness on the electrical properties of invar36 thin film for strain gauge applications," *International Journal of Thin Film Science and Technology*. Vol. 2 : Iss. 3 , Article 1.

Available at: <https://digitalcommons.aaru.edu.fo/ijtfst/vol2/iss3/1>

This Article is brought to you for free and open access by Arab Journals Platform. It has been accepted for inclusion in International Journal of Thin Film Science and Technology by an authorized editor. The journal is hosted on [Digital Commons](#), an Elsevier platform. For more information, please contact rakan@aar.edu.fo, marah@aar.edu.fo, u.murad@aar.edu.fo.

Influence of annealing and thickness on the electrical properties of invar36 thin film for strain gauge applications

H. M Kalpana^{1,*}, V. Siddeswara Prasad¹ and M. M Nayak²

¹ Department of Instrumentation Technology, Siddaganga Institute of Technology, Tumkur 572103, Karnataka, India

² Centre for Nano Science and Engineering, Indian Institute of Science, Bangalore 560 012, India

Received: 27 Jul. 2013, Revised: 4 Aug. 2013, Accepted: 6 Aug. 2013

Published online: 1 Sep. 2013

Abstract: Invar36 thin films with various thicknesses from 200 Å to 1400 Å are deposited on glass substrates by DC magnetron sputtering technique. After deposition, the samples are annealed in vacuum ambient (10^{-5} mbar) upto 500°C. Electrical properties of as-deposited as well as annealed films are analyzed with respect to thickness and annealing temperature. In situ measurement of sheet resistance of films with respect to annealing temperature is carried out by four probe technique. There is a decrease of sheet resistance and resistivity of all films with increasing temperature irrespective of film thickness. The resistivity of the as deposited films is around 230 $\mu\Omega$ -cm and decreases with increasing temperature and found as 84 $\mu\Omega$ -cm for 550 Å film annealed at 500°C. Temperature co-efficient of resistance (TCR) of films at different temperature is measured and is found to be in the range of $10^{-4}/^{\circ}\text{C}$. Gauge factors of as deposited and annealed at 300°C and 500°C films are measured by using four point bending technique and it is found that gauge factor decreases with respect to annealing temperature irrespective of film thickness. The best characteristics among different thickness and annealing temperature are obtained at 500°C, for the films of thicknesses between 400 Å to 600 Å.

Keywords: DC magnetron sputtering, Invar36 thin film, Annealing, TCR, Gauge factor, Strain gauge

1 Introduction

Fe-Ni alloy with Ni concentration of around 36% also known as invar36 alloy exhibits low coefficient of thermal expansion (CTE) and high dimensional stability near room temperature [1]. Due to their low CTE and soft magnetic properties, these alloys are used in many industrial applications [2]. Typical examples of applications include: thermostatic bimetals, glass sealing, integrated circuit packaging, cathode ray tube shadow masks, composite molds/tooling and membranes for liquid natural gas tankers [3]. In addition to general applications, in recent year's invar36 alloy in thin film form is gaining importance in sensors as well as in micro electro mechanical system applications [3,4,5]. Thin film technology plays an important role in the mass fabrication of thin film strain gauges with considerable cost reduction [6,7]. Sputtering is one of the vacuum deposition techniques used to prepare thin film strain gauges. It has many advantages. They are high uniformity of thickness of the deposited films, good adhesions to the substrate, better reproducibility of films, ability of the deposit to maintain the stoichiometry of the original target composition and relative simplicity of film thickness control [8]. An ideal strain gauge for measurement purposes should possess fairly good strain sensitivity, low temperature coefficient of resistance (TCR) and excellent thermal stability [9,10]. Selection of strain gauge material to meet the above said properties is very important. This paper describes the experimental work carried out on invar36 thin film to make use of the same for strain gauge application. Sputter deposited invar36 films possess stresses that are caused by thermal strain mismatch or by lattice parameter mismatch. In order to minimize residual stress of thin films and to prevent the drift in electrical properties of thin film devices, post annealing is very essential. The effect of annealing temperature as well as film thickness on variations of TCR, resistivity and gauge factor of invar36 thin film for strain gauge applications are systematically analyzed.

* Corresponding author e-mail: hm_kalpanaravi@yahoo.co.in

2 Experimental Work

The target is an invar36 foil of 50mm diameter and 0.2mm thick (procured from ESPI Metals) bonded on copper disc of diameter 50mm and 6mm thick by using silver paste. Related data of invar36 alloy are given in Table 1. Glass slides of $75\text{mm} \times 25\text{mm} \times 1.5\text{mm}$ dimensions are used as substrates to deposit invar36 thin films. Substrate preparation is the key issue in the fabrication sequence. Its importance became apparent through its relation to the adhesion and quality of the film. Glass slides are cleaned with detergent to remove dirt and foreign particles. Organic contents present on the surface of glass slides are removed by acetone ultrasonic bath. Glass slides are degreased with vapors of isopropyl alcohol. At each stage glass slides are washed with deionised water and finally they are dried by blowing nitrogen gas [5]. Invar36 thin films are deposited on glass slides by DC magnetron sputtering technique at room temperature. Planar RF/DC

Table 1: Related data of invar36 alloy

Thickness	0.2mm
Diameter	50mm
Composition	Ni 35.9%, Fe Balance, Cr 0.03%, Mn 0.3%, Si 0.07%, Al < 0.005%, P < 0.002%, S < 0.001%, C 0.002%

Magnetron Sputtering Unit comprising of diffusion pump backed by a rotary pump is used for deposition of invar36 thin film. The cleaned substrate and target are fixed to substrate holder and target holder respectively housed in a deposition chamber which is evacuated to a pressure of 1×10^{-5} mbar with the help of rotary and diffusion pump combination. The extraneous gas constituents present in it is removed by repetitive flushing with high purity (99.999%) argon gas [5]. Then it is filled with argon gas to obtain a working pressure of 1×10^{-2} mbar. Foreign particles, if present any on the target surface are removed by Pre-sputtering for 5 to 10 minutes by closing the shutter over the substrate. Several experiments are conducted to optimize the deposition parameters. Deposition rate is found by measuring the thickness of invar36 thin film using surface profilometer. The average deposition rate is found to be 18nm/min. Optimized sputtering parameters used for the preparation of test samples are tabulated in Table 2. Invar36 thin films of various thicknesses (200-1400Å) are

Table 2: Optimized sputtering parameters

Distance between target & substrate	50 mm
Base pressure	1×10^5 mbar
Working pressure	1×10^2 mbar
DC voltage	330 V
DC current	70 mA

deposited on glass slides by varying deposition time. A precision rectangular mechanical mask of $20\text{mm} \times 1\text{mm}$ prepared using a CNC (Computer Numerically Controlled) spark erosion machine with a dimensional tolerance of $\pm 1\mu\text{m}$ is utilized to deposit invar36 thin films. Annealing of the samples is carried out in a vacuum system. Samples are held in horizontal position by a special jig (the substrate holding and heating arrangement). A k type thermocouple is installed with the arrangement for temperature sensing. A PID controller with $\pm 1^\circ\text{C}$ tolerance is employed as temperature controller. The samples are annealed in vacuum (10^{-5} mbar) for one hour at temperatures of 300°C and 500°C . The heating rate is $2-3^\circ\text{C}/\text{min}$, and the cooling rate is $1^\circ\text{C}/\text{min}$. In situ measurement of sheet resistance and temperature coefficient of resistance (TCR) of films with respect to different temperatures are carried out by four-probe method with the help of current source meter (Keithley 6221) with accuracy of $\pm 0.05\%$ resolution of 100 nA and Nano voltmeter (Keithley 2182A) with 0.05% accuracy and 10 nV resolution. A constant current of about 1 mA from current source is passed through the sample and the voltage drop across the same is measured using the nano voltmeter. The linear portion of the sheet resistance - temperature variation obtained during cooling is preferred to calculate the TCR value, because it is reversible up on repeated heating and cooling indicating the stabilized condition of the film [11]. The TCR of film is calculated using equation (1)

$$TCR = \frac{\Delta R}{R(\Delta T)} \quad (1)$$

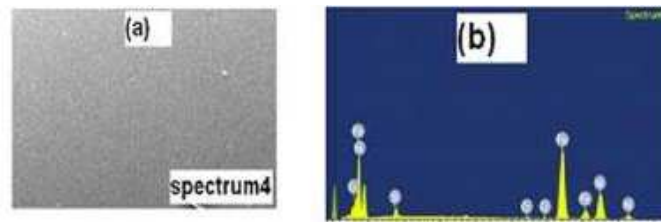


Fig. 1: (a) SEM image of invar36 thin film (b) EDX spectrum of invar36 thin film

Where ΔR corresponds to a small change in sheet resistance and ΔT is small change in temperature. A four point bending setup is designed and fabricated in order to study the resistance-strain behavior of films and hence to measure the gauge factor of the films [5]. Four point bending setup is calibrated at room temperature with overall accuracy of 0.21% by using metal foil strain gauges of known gauge factor values (2.1). In this arrangement the glass slides with deposited invar36 film are held between four rolling pins, two at the top and two at the bottom. This allows the equal and opposite couples to both ends of the sample. The strain (ϵ) experienced by the film is calculated using equation (2).

$$\epsilon = \frac{4t|\delta|}{d^2} \quad (2)$$

Where 't' is the thickness of the glass slide and 'd' is the distance between the rolling pins. δ is the deflection in μm at the center of the substrate measured by Mitutoyo dial indicator-21095-10 with 1μ resolution. Simultaneously the relative change in resistance ($\Delta R/R$) is measured using calibrated $6\frac{1}{2}$ digit Hewlett Packard (model HP34401A) digital multimeter. The value of gauge factor is calculated using equation (3)[5].

$$GF = \frac{\frac{\Delta R}{R}}{\epsilon} \quad (3)$$

3 Results and Discussion

Energy Dispersive X-Ray (EDX) Spectrum of invar36 thin film collected from scanning electron microscope (JEOL JSM-5600LV) is shown in Fig.1(a). A representative EDX spectrum collected from the bottom right side (Spectrum4) of the sample is shown in Figure 1(b). The EDX analysis indicates that the main compositions of invar36 thin film are Fe and Ni and presence of small amounts of silicon and chromium also. These results show that the composition of film is almost same as of the bulk foil as given in Table 1 (supplied by ESPI metals). Elements which are present in smaller percents are not traced because of different sputtering yields. Since structural and electrical properties are dependent on the composition of film and it is very important to obtain the accurate values of them. The average compositions of Fe and Ni are found as 59.40% and 34.94% which are in the invar36 region; hence it is possible to obtain stable and low CTE films with good electrical and structural properties for strain gauge applications.

Sheet resistance measurements are carried out by varying the temperature at the rate of $2\text{-}3^\circ\text{C}/\text{min}$ from room temperature to annealing temperature (500°C). Variation of sheet resistance of one of the sample ($\sim 650 \text{ \AA}$) with temperature during both heating and cooling cycles is as shown in Fig. 2. The arrows indicate the variation of film sheet resistance as the temperature is increased and decreased. Initially sheet resistance of film remains almost constant from room temperature to 80°C (portion AB). It is observed that after 80°C sheet resistance decreases slowly (portion BC) upto 250°C because of decrease of the number of structural defects induced in film during the deposition process and decreases more rapidly after that (portion CD). This may be because of the beginning of the recrystallization process. From 350°C sheet resistance decreases slowly and reaches a minimum value (E) at 500°C because of densification of the film with accompanied grain growth and micro pore vanishing. The rate of decrease of sheet resistance is slow at beginning and fast at higher temperatures. The observed decrease of sheet resistance with temperature shows that the contribution to the resistance due to the removal of the defects is greater than that to thermal vibration of the lattice. Heating is stopped after observing the minimum and the film is allowed to cool to room temperature (portion EF). It is evident that the change in sheet resistance is very small when the temperature is decreased from 500°C to room temperature (30°C).

The experiment is repeated several times and the variation of sheet resistance is observed to follow the same path from (F) to (E) and back to (F) indicates that sheet resistance is linear and retraceable with temperature. This indicates the

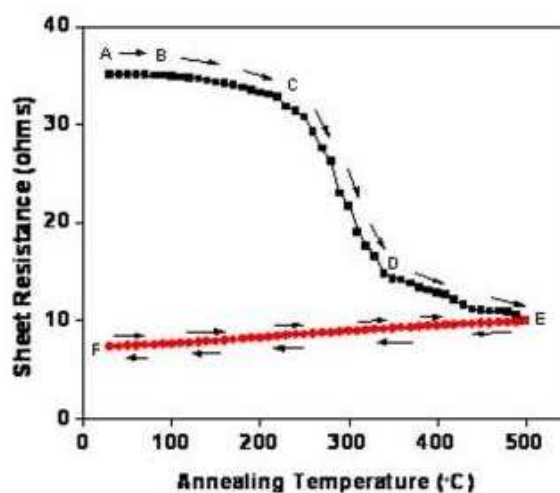


Fig. 2: Variation of sheet resistance with temperature of invar36 thin film

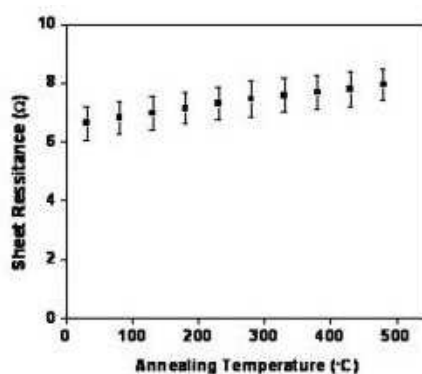


Fig. 3: Variation of mean sheet resistance and associated error of invar36 thin film with temperature

completely annealed and stabilized condition of the film. The observed resistance temperature behavior is similar to that found in case of common metallic films [10, 11]. The average standard deviation during cooling from 500 °C to 30 °C is found around ± 0.5 . Fig.3 depicts the standard error generated for the mean value of the variation of sheet resistance with decreasing temperature after first thermal cycle. For the sake of legibility only few points are shown. The value of error calculated found within ± 0.3 which indicates stability of the sheet resistance of the film after annealing. Since films are vacuum annealed there is no oxidation effects on sheet resistance is observed.

Variation of sheet resistance of as deposited and films annealed at 300 °C and 500 °C with thickness is shown in Fig.4. It is observed that sheet resistance decreases with increasing film thickness at all temperature [12]. It is evident from the fig.4 that the variation of sheet resistance with thickness is similar to that of metallic films [13]. It is also observed that as the film is thin the sheet resistance is very high and as the thickness increases it decreases fast upto 400 Å and after 500 Å the variation of sheet resistance with increase of film thickness is less. The smaller variation of sheet resistance at higher film thickness is attributed to higher uniformity of the film compared to films of lower thickness.

Variation of film resistivity with thickness at different temperatures is shown in Fig.5. It is observed that at lower film thickness the variations of resistivity is more as compared to films of higher thickness because of electron scattering by surface is more at lower thickness [13]. The impurities and structural defects formed during film deposition reduce the electron mean free path and increase the film resistivity [14]. Defects can be removed by annealing the films which reduces the resistivity as indicated from Fig.5. For film of 550 Å thickness annealed at 500 °C the resistivity obtained is $84 \mu\Omega\text{-cm}$ which is almost equal to the bulk value ($81 \mu\Omega\text{-cm}$) [15].

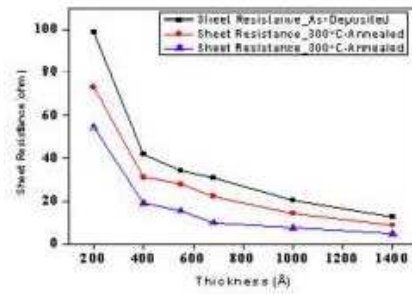


Fig. 4: Variation of sheet resistance with thickness at different annealing temperature

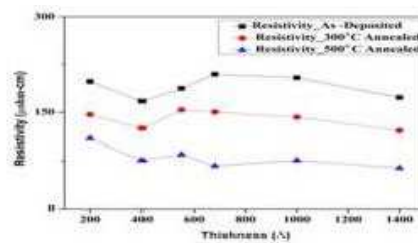


Fig. 5: Variation of resistivity with thickness at different annealing temperature

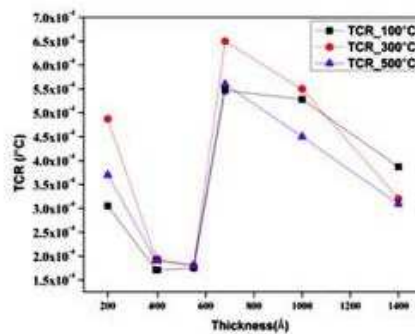


Fig. 6: Variation of TCR with thickness at different annealing temperature

Linear portion (EF) obtained during cooling shown in Fig.2 is used to calculate TCR value of invar36 thin film. The linear portion is preferred to calculate the TCR value because it is reversible on repeated heating and cooling, indicating the completely annealed condition of the film [10]. TCR of annealed samples are calculated from 100°C, 300°C and 500°C to 30°C and plotted against thickness shown in Fig.6. TCR value varies with temperature as well as thickness. In the thickness range of 400Å to 600Å, TCR value obtained at 100°C, 300°C and 500°C are $1.71 \times 10^{-4}/^{\circ}\text{C}$, $1.8 \times 10^{-4}/^{\circ}\text{C}$, $1.9 \times 10^{-4}/^{\circ}\text{C}$ respectively. These values are lesser than the available results and hence suitable for the construction of strain gauges [5].

Variation of gauge factor of as deposited as well as annealed invar36 thin films at 300°C and 500°C with film thickness is shown in Fig.7. There is no significant differences in gauge factor values of as deposited and films annealed at 300°C as indicated in Fig.7. It is also observed that gauge factor value decreases remarkably when the films are annealed at 500°C compared to as deposited and annealed at 300°C films. This is because of sharp decrease of sheet resistance when the temperature is increased above 300°C as shown in Fig.2. The variations of sheet resistance with annealing temperature and the influence of the same on resistivity, TCR as well as the gauge factor of the film is due to the structural changes of the film with annealing. Atomic force microscopy (AFM) is carried out to illustrate the effect of annealing on the surface morphology and grain growth, which is the main cause for the decrease of sheet resistance with annealing at different

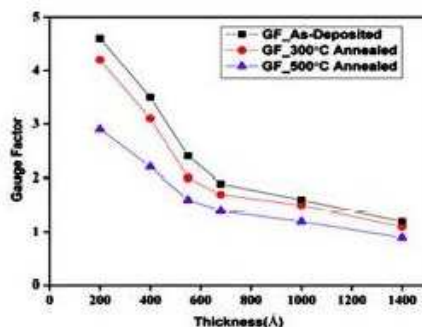


Fig. 7: Variation of Gauge Factor with thickness at different annealing temperature

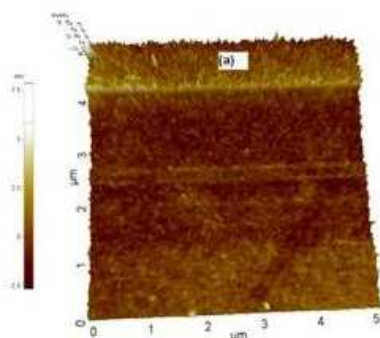


Fig. 8: Surface morphology of invar36 thin films (a) as-deposited

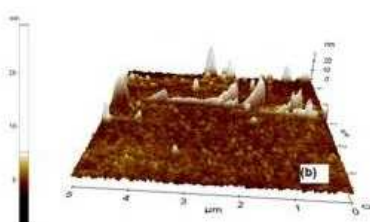


Fig. 9: Surface morphology of invar36 thin films (b) annealed at 300°C

thickness of the film. Fig.8, Fig.9 and Fig.10 illustrates the AFM images of invar36 thin films of $\sim 550\text{\AA}$ thickness in as-deposited, annealed at 300°C and 500°C carried out in contact mode using AFM Xe-70 Park system. All films are scanned through $5\text{mm} \times 5\text{mm}$ area. It is observed from AFM images that there is an increase of grain growth with annealing temperature. The calculated values of root mean square (RMS) roughness values of the as-deposited and annealed at 300°C and 500°C film are found as 0.825nm, 1.661nm, 12.25nm, respectively. It is evident from the results that the film annealed at 500°C exhibits highest roughness value as compared with as-deposited and films annealed at 300°C [16]. The increase in roughness is due to the migration of the surface atoms and release of stress in the film [17, 18]. This is also attributed to the aggregation of faceted grains with voids.

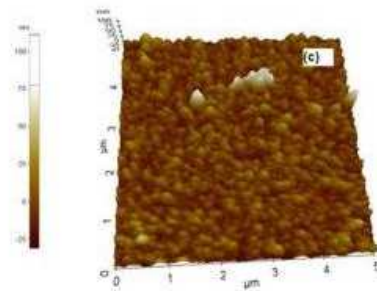


Fig. 10: Surface morphology of invar36 thin films (c)annealed at 500°C

4 Conclusions

Experimental investigations are carried out on the thickness and annealing effects on electrical properties of invar36 thin films. From this study it is observed that annealing of invar36 thin films brings about relatively favorable changes in electrical properties of films for their possible application as strain gauges. The value of resistivity obtained decreases with annealing and approaches the bulk value ($81\mu\Omega\text{-cm}$) for film annealed at 500°C. TCR values obtained for annealed films irrespective of thickness are in the range of $10^{-4}/^{\circ}\text{C}$, which is very less compared to available results. Even though gauge factor values obtained for annealed films are lesser than as deposited films, they are preferable since they are more stable than other films. AFM analysis of $\sim 550\text{\AA}$ thick film also reveals the effect of annealing on surface morphology, grain growth which intern influences the electrical properties. Annealing had an effect on all properties of invar36 thin films and the effect is particularly noticeable for films of lower thickness. It can be concluded that annealed invar36 thin film in the thickness range from 400Å to 600Å are preferable for thin film strain gauge applications.

Acknowledgement

The authors are grateful to Siddaganga Institute of Technology, Tumkur 572103, Karnataka, India, for supporting this research work.

References

- [1] B. Jinan, Al-Dabbagh, K. Ismail, Al-Faluji, Yusof Bin Hashim, International Journal of Engineering and Science, **1**, 48-51 (2012).
- [2] R. R. Mulyukov, V. A. Kazantsev, Kh. Ya. Mulyukov, A.M. Burkhanov, I.M. Safarov, I. Kh. Bitkulov, Rev. Adv. Mater. Sci., **11**, 116-121 (2006).
- [3] J. L. McCrea, G. Palumbo, G. D. Hibbard, U. Erb, Rev. Adv. Mater. Sci., **5**, 252-258 (2003).
- [4] Anand Kumar Dokania, B. Kocdemir, U. Herr, Thermal expansion of invar thin film for MEMS application. International Symposium of Research Students on Material Science and Engineering, Chennai, India, 20-22 (2004).
- [5] K. Rajanna, M. M. Nayak, Materials Science and Engineering, **B77**, 288-292 (2000).
- [6] R. John Stephen, K. Rajanna, Vivek Dhar, K. G. Kalyan Kumar, S. Nagabushanam, IEEE Sensors Journal, **4**, 373-377 (2004).
- [7] H. Imam, P. M. Kazi, T. N. Wild, M. Moore, Sayer, Thin Solid Films, **515**, 2602-2606 (2006).
- [8] G. R. Witt, Thin Solid Films, **22**, 133-156 (1974).
- [9] K. Rajanna, S. Mohan, E. S. R. Gopal, Indian Journal of Pure & Applied Physics, **27**, 453-460 (1989).
- [10] K. Rajanna, S. Srinivasulu, M. M. Nayak, S. Mohan, Journal of Materials Science Letters, **12**, 37-39 (1993).
- [11] K. Rajanna, G. K. Muralidhar, K. G. M. Nair, T. Panchapagesan, M. M. Nayak, S. Mohan, Journal of Applied Physics, **76**, 3573-3578 (1994).
- [12] M. Urse, A. E. Moga, M. Grigoras, Journal of Optoelectronics and Advanced Materials, **6**, 629-632 (2004).
- [13] P. Mohan, K. Schwarz, D. Wagner, The American Physical Society, (1991).
- [14] F. Wang, M. Z. Wu, Y. Y. Wang, Y. M. Yu, X. M. Wu, L. J. Zhuge, Vacuum, **89**, 127-131 (2013).
- [15] M. Konno, H. Konno, Journal of Magnetism and Magnetic Materials, **118**, 381-386 (1993).
- [16] Y. M. Yeh, G. C. Tu, T. H. Fang, Journal of Alloys and Compounds, **372**, 224-230 (2004).
- [17] Wu Tang, Kewei Xu, Ping Wang, Xian Li, Microelectronic Engineering, **66**, 445-450 (2003).
- [18] V. Ng, J. F. Hu, A. O. Adeyeye, J. P. Wang, T. C. Chong, Journal of Applied Physics, **91**, 7206-7208 (2002).